Sains Malaysiana 43(6)(2014): 885–894

Nano Fe_3O_4-Activated Carbon Composites for Aqueous Supercapacitors

(Nanokomposit Fe_3O_4-Karbon Aktif untuk Super-Kapasitor Akueus)

M.Y. Ho, P.S. Khiew*, D. Isa, T.K. Tan , W.S. Chiu, C.H. Chia, M.A.A. Hamid & R. Shamsudin

ABSTRACT

In this study, a symmetric supercapacitor has been fabricated by adopting the nanostructured iron oxide (Fe_3O_4)-activated carbon (AC) composite as the core electrode materials. The composite electrodes were prepared via a facile mechanical mixing process and PTFE polymeric solution has been used as the electrode material binder. Structural analysis of the nanocomposite electrodes were characterized by scanning electron microscopy (SEM) and Brunauer-Emmett-Teller (BET) analysis. The electrochemical performances of the prepared supercapacitor were studied using cyclic voltammetry (CV) and electrochemical impedance spectroscopy (EIS) in 1.0 M Na_2SO_3 and 1.0 M Na_2SO_4 aqueous solutions, respectively. The experimental results showed that the highest specific capacitance of 43 F/g is achieved with a fairly low Fe_3O_4 nanomaterials loading (4 wt. %) in 1 M Na_2SO_3. It is clear that the low concentration of nanostructured Fe_3O_4 has improved the capacitive performance of the composite via pseudocapacitance charge storage mechanism as well as the enhancement on the specific surface areas of the electrode. However, further increasing of the Fe_3O_4 content in the electrode is found to distort the capacitive performance and deteriorate the specific surface area of the electrode, mainly due to the aggregation of the Fe_3O_4 particles within the composite. Additionally, the CV results showed that the Fe_3O_4/AC nanocomposite electrode in Na_2SO_3 electrolyte exhibits a better charge storage performance if compared with Na_2SO_4 solution. It is believed that Fe_3O_4 nanoparticles can provide favourable surface adsorption sites for sulphite (SO_3^{2-}) anions which act as catalysts for subsequent redox and intercalation reactions.

Keywords: Activated carbon; aqueous electrolyte; iron oxide; supercapacitor

ABSTRAK

Dalam kajian ini, super-kapasitor bersimetri telah dibina dengan menggunakan nanokomposit ferum oksida (Fe_3O_4)-karbon aktif (AC) sebagai bahan asas elektrod. Elektrod nanokomposit telah disediakan secara percampuran mekanikal mudah dan larutan polimer PTFE telah digunakan sebagai agen pengikat untuk bahan elektrod. Pencirian struktur elektrod nanokomposit telah dilakukan dengan mikroskopi pengimbasan elektron (SEM) dan analisa Brunauer-Emmett-Teller (BET). Pencapaian elektro-kimia untuk super-kapasitor dalam larutan akueus 1.0 M Na_2SO_3 dan 1.0 M Na_2SO_4 telah dianalisis dengan mengunakan voltametri siklik (CV) dan spektroskopi impedansi elektro-kimia (EIS). Keputusan kajian menunjukkan kemuatan kapasitan tertinggi sebanyak 43 F/g boleh dicapai dengan penambahan kecil nanozarah Fe_3O_4 dalam larutan 1 M Na_2SO_3. Ini jelas menunjukkan penambahan nanozarah Fe_3O_4 pada kandungan yang rendah dapat meningkatkan pencapaian kemuatan kapasitan elektrod komposit menerusi mekanisme caj penyimpanan pseudo-kapasitan dan juga menambahkan keluasan permukaan spesifik elektrod. Walau bagaimanapun, penambahan kandungan Fe_3O_4 yang lebih tinggi di dalam elektrod didapati akan menjejaskan pencapaian kapasitan dan mengurangkan keluasan permukaan spesifik elektrod, disebabkan penggumpalan nanozarah Fe_3O_4 di dalam komposit. Tambahan pula, keputusan CV menunjukkan pencapaian caj penyimpanan elektrod nano-komposit Fe_3O_4/AC dalam elektrolit Na_2SO_3 adalah lebih baik berbanding dengan larutan Na_2SO_4. Nanozarah Fe_3O_4 dipercayai dapat menyediakan tapak penjerapan anion sulfida (SO_3^{2-}) yang bertindak sebagai pemangkin untuk tindak balas interkalasi dan redoks seterusnya.

Kata kunci: Elektrolit akueus; karbon aktif; nanozarah ferum oksida; super-kapasitor

Introduction

Global warming, air-pollution emission, rising oil prices and fossil fuel depletion have received critical attention in the new global economy in which a progressive swing from an oil-based economy to an electricity-based civilization is observed (Pasquier et al. 2003). Transforming natural energy from sustainable and renewable resources such as the sun, ocean tides and wind could yield high electricity energy output. However, man has limited control over the natural phenomena due to the climate/geographical constraints. For these reasons, energy storage technology appears as one of the most promising options in tackling the problem since renewably-generated electrical energy can be stored during the optimum period for future use.

Electrochemical capacitor, also known as supercapacitor, is a unique energy storage device designed for high power density, high charge-discharge cycle life and high discharge efficiency (Wu 2002). It differs from

conventional capacitor by storing charge using the double layer concept in which charge accumulation occurs at the interface between electrode and electrolyte via the double-layer charging effects. The additional contribution of pseudo capacitance may also be part of the observed capacitance due to some participation of functional groups present on the electrode surface in redox reactions or chemisorption processes involving partial charge transfer (Conway et al. 2007).

On the basis of electrode materials used and the charge storage mechanisms, the core electrode material of supercapacitor generally can be classified into three main categories: Carbon materials with high surface area, such as activated carbon and carbon aerogel; transition metal oxides such as RuO_2, NiO_2, MnO_2, Fe_3O_4 and conducting polymers such as polyaniline and polypyrrole (Kalpana et al. 2006; Wang et al. 2009; Zhang & Chen 2008). The carbon systems employ the double layer storage mechanism involving the charge separation at the interface between the carbon electrode and electrolyte. No charge transfer takes place across the interface of the electrode material. For this reason, this process is non-Faradaic in nature and therefore we classify the carbonaceous materials as electric double layer capacitor or EDLC (Cottineau et al. 2005). In contrast, the charge storage mechanism achieved by the transition metal oxides and conducting polymers is Faradaic in nature. The redox reaction between electrode materials and electrolyte ions in the appropriate voltage window gives rise to the pseudo-capacitance through the electron transfer that is produced from the oxidation state changes, according to Faraday's laws (Shukla et al. 2000).

Over the past few years, significant effort has been devoted to the fabrication of advanced nanostructured metal oxides as the core electrode material, especially on hydrous $RuO_2.xH_2O$ (Hu & Chen 2004; Hu et al. 2007; Kim & Popov 2002). RuO_2 is widely studied because it is conductive and has three accessible distinct oxidation states. The pseudo-capacitive behaviour of RuO_2 in acidic solutions has been the focus of research in the past 30 years (Simon & Gogotsi 2008). Although $RuO_2.nH_2O$ gives high specific capacitance, its application has been hindered by its high cost (Du et al. 2009). Therefore, there is a need to search for less expensive pseudocapacitance materials to support the growing demand on supercapacitor in manufacturing industry, as a result of rapid advancement of consumer electronic products and technology. A number of research studies have shown an increasing interest in other transition metal oxides with various oxidation states, such as NiO (Ganesh et al. 2006; Nathan et al. 2008; Yeong et al. 2005; Yuan et al. 2005), MnO (Belanger et al. 2008; Lee & Goodenough 1999; Nagarajan et al. 2006), SnO_2 (Jayalakshimi et al. 2007; Kuo & Wu 2003; Lu et al. 2010), Fe_2O_3 (Mallouki et al. 2006; Nagarajan & Zhitomirsky 2006; Xie et al. 2011) and Fe_3O_4 (Brousse & Belanger 2003; Chen 2009; Wu et al. 2003).

Iron oxides have been identified as the potential electrode materials in view of the low-cost and environmentally friendly nature. Recently, large capacitance exhibited by iron powder electrodes has been reported in alkali sulphite and sulfate solutions (Brousse & Belanger 2003; Chen 2009; Dubal et al. 2012; Nagarajan & Zhirtomirkey 2006; Sassin et al. 2010; Wang et al. 2008, 2006; Xie et al. 2011). Wu (2002) firstly reported that Fe_3O_4-SnO_2 composite electrode can achieve a specific capacitance of 33 F/g in 1.0 M Na_2SO_4 aqueous solution. It is suggested that the low conductivity of Fe_3O_4 combined with other conductive materials such as SnO_2 is essential to obtain large capacitance. In order to identify the effect of different electrolytes on Fe_3O_4 electrodes, Wu et al. (2003) also have prepared an electrode that is consisted of a mixture of Fe_3O_4 (90 wt. %), CB (10 wt. %), PTFE (4 wt. %) via coprecipitation method. The specific capacitances of the composite electrode are found to be 38, 5.3, 4.9, 5.8 F/g in 1 M Na_2SO_3, 1 M Na_2SO_4, 1M NaCl and 1M KOH respectively.

The findings of these two studies (Wu 2002; Wu et al. 2003) are consistent with another investigation on capacitive mechanism of Fe_3O_4 in Na_2SO_3, Na_2SO_4 and KOH aqueous (Wang et al. 2006) and suggested that the capacitance of the oxide was found to be sensitive to the anion species. The experimental results indicated that Fe_3O_4 electrodes in Na_2SO_3 exhibit the highest specific capacitance value (170 F/g), followed by Na_2SO_4 (25 F/g) and KOH (3 F/g). In the work of Du et al. (2009), they reported the capacitive characteristic of nanostructured Fe_3O_4-AC based asymmetric supercapacitor in 6 M KOH solution. This hybrid system (a positive Fe_3O_4 electrode and a negative AC electrode) is found to deliver a specific capacitance of 37.9 F/g within potential range of 0-1.2 V. A composite supercapacitor containing Fe_3O_4 nanoparticles dispersed in multiwalled carbon nanotubes (MWNTs) was reported by Kim and Park (2011). The Fe_3O_4/MWNTs composite electrode exhibits specific capacitance of 165 F/g in 1 M Na_2SO_3, which this value is almost 3-fold enhancement if compared to the pure MWNT electrode (58 F/g).

To our best knowledge, there have been few investigations on Fe_3O_4/AC nanocomposite supercapacitor to date. In this work, we explore the nanostructured Fe_3O_4/AC composite as the core electrode materials via simple facile mechanical mixing method for the first time. Although the poor electric conductivity of Fe_3O_4 limits its application in high power storage devices, the incorporation of carbon black can improve the electrochemical performance of the Fe_3O_4 loading composite electrodes.

Materials and Methods

Preparation of Electrodes

Active materials were made by doping different amount of Fe_3O_4 nanopowder (Sigma Aldrich, particle size < 50 nm, BET surface ~ 38 m^2g^{-1}) to AC nanopowder (Sigma Aldrich, BET surface ~ 900 m^2g^{-1}) to form composite

electrodes, containing carbon black powder (Ketjenblack, EC-600JD from Akzo Nobel, surface area ~ 1400 m^2/g) and polytetrafluoroethylene (PTFE) in the weight ratio of 80:15:5. The mixture was dissolved into a 1:1 mixed solution of distilled water and isopropanol. Fifteen wt. % carbon black was added to increase the electrode conductivity of Fe_3O_4 nanopowder (Du et al. 2009). The mixtures in dough form were then cold rolled into 0.8 mm thick films. Electrodes were punched into coin-shaped electrodes of 2 cm^2 and were dried in a vacuum oven at 80°C for 45 min to ensure the isopropanol solvent was evaporated completely. After being immersed overnight in 1 M Na_2SO_3 and 1 M Na_2SO_4, respectively, the discs were then mounted onto a stainless steel-current collector in a Teflon cell holder by means of screw-fitting plug for electrochemical measurements.

STRUCTURAL ANALYSIS

The surface morphology of the composite was observed using a field-emission scanning electron microscope (FESEM, FEI, Quanta 400 F). Five-point surface area measurement using Brunauer-Emmett-Teller (BET) was made with a Micromeritic, ASAP 2020 surface area analyzer under N_2 gas.

ELECTROCHEMICAL CHARACTERIZATION

Electrochemical tests including cyclic voltammogram (CV) and electrochemical impedance spectroscopy (EIS) were performed using Nova software in Autolab potentiostat (model: PGSTAT128N). In this study, all electrodes were tested in 1 M Na_2SO_3 and 1 M Na_2SO_4 solutions that were prepared by dissolving the appropriate amount of Na_2SO_3 and Na_2SO_4 salts, respectively, in deionized water. The respective specific capacitances (C_s) were determined by using half integrated area of CV curve to obtain the charge (Q) and subsequently dividing the charge by the mass of the electrode (*m*) and the width of the potential window (ΔV) following equation: $C_s = Q/m\ \Delta V$.

RESULTS AND DISCUSSION

MICROSTRUCTURAL CHARACTERIZATION

Scanning electron micrographs in Figure 1(a) to 1(f) indicates different amount of iron oxide loaded onto the composite electrodes. SEM photograph 1(a) and 1(b) show that the pitted and fragmented surfaces are more prominent for the pure AC and 4 wt. % Fe_3O_4 composite electrodes while the formation of compact and rigid surface structures are observed for samples with increasing Fe_3O_4 loading, as depicted in SEM photograph 1(e) and 1(f). SEM photograph 1(a) and 1(b) show that the pitted and fragmented surfaces are more prominent for the pure AC and 4 wt. % Fe_3O_4 composite electrodes while the formation of compact and rigid surface structures are observed for samples with increasing Fe_3O_4 loading, as depicted in SEM photograph 1(e) and 1(f). The compact surface contour will retard the ion diffusion to the porous AC electrode, resulting in the loss of overall capacitance of the composite electrodes, as depicted in Table 2. The present findings seem to be consistent with other research study, which found that increasing the amount of ruthenium oxide would decrease the surface roughness of the composite electrodes and subsequently distort the specific capacitance (Kim & Popov 2002).

In order to elucidate the porosity property of the electrode, BET analysis has been conducted. The BET surface areas of the samples are summarized in Table 1. The BET analysis showed that the addition of 4 wt. % Fe_3O_4 increases the specific surface area of pure AC electrode from 916 to 949 m^2g^{-1} and thus improves the capacitive performance improvement of the composite electrode effectively. This observation is in good accordance to research finding by Zhang and Chen (2008), which clearly indicate that the enhanced capacitance is mainly attributed to the high surface area of the core electrode material. On the other hand, further increase of Fe_3O_4 compound to 60 wt. % causes the specific surface area of the composite electrode decreased to 800 m^2g^{-1} or 15.7% surface area reduction. The specific surface area of pure Fe_3O_4 (38 m^2g^{-1}) is lower than that of the AC; when the Fe_3O_4's content is increased, the specific surface area of the composite decreases. Fe_3O_4 nanopowders probably gathered to form agglomerates within AC electrodes as shown in Figure 1(f). The crystal growth of Fe_3O_4 reduces the ionic migration and thus causes the increase in diffusion path length. A fade in capacitance as a result of reduced surface area has been reported by several researchers in similar application (Hu & Chen 2004; Kim & Popov 2002).

ELECTROCHEMICAL CHARACTERIZATION

Cyclic Voltammogram (CV) Figures 2 and 3 show the CV plots for the Fe_3O_4/AC nanocomposite electrodes with different Fe_3O_4 loading in 1 M Na_2SO_3 and 1 M Na_2SO_4 electrolytes, respectively, at a constant scan rate of 10 mV s^{-1}. It can be seen that the voltammograms for the samples are not symmetrical along the current axes, especially in Na_2SO_3 solution. The fact that the voltammograms do not show perfect rectangular features with a mirror image characteristic implies that there is a substantial pseudocapacitance contribution to the overall measured capacitance. In this study, it can be seen that the current response of the 4 wt. % Fe_3O_4 electrodes in 1 M Na_2SO_3 electrolyte is found to be greater than those of AC electrode and other composite electrodes, suggesting that highest specific capacitance is achieved for such composition. It is believed that the presence of Fe_3O_4 nanoparticles in AC electrodes can provide favourable surface adsorption sites for sulphite anions which act as catalysts for subsequent redox and intercalation reactions. Interestingly, the types of electrolyte actually is playing a vital role in this context since the CV performance of the electrode material in Na_2SO_4 solution is found to be

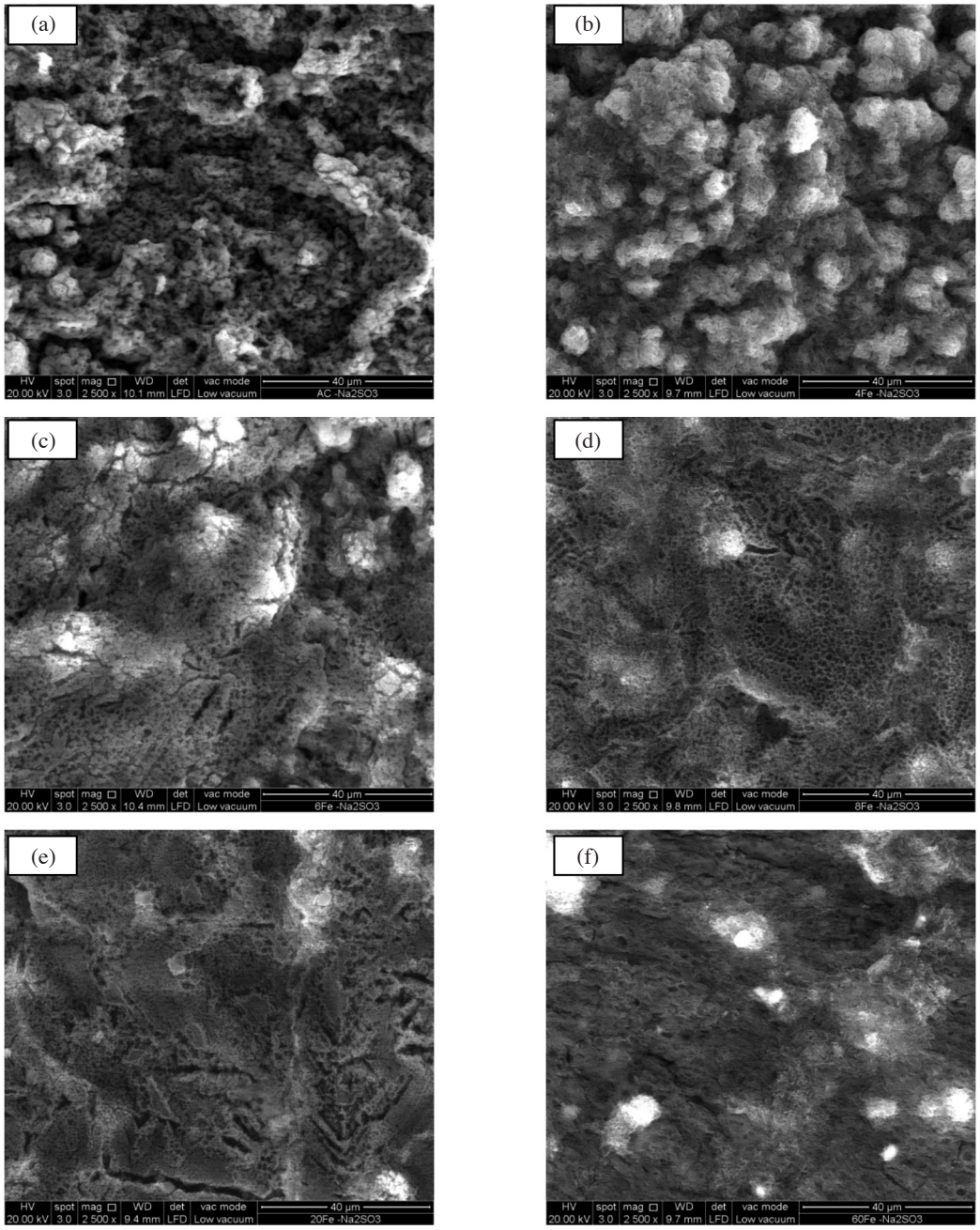

FIGURE 1. Scanning electron micrographs of different Fe_3O_4 loading in AC electrodes: (a) AC, (b) 4 wt. % Fe_3O_4, (c) 6 wt. % Fe_3O_4, (d) 8 wt. % Fe_3O_4, (e) 20 wt. % Fe_3O_4, (f) 60 wt. % Fe_3O_4

TABLE 1. BET surface area of Fe_3O_4-AC composite electrodes

Electrode material	BET surface area (m^2/g)
CB	1338.44
AC	916.00
4 wt. % Fe_3O_4/AC/CB	949.03
8 wt. % Fe_3O_4/AC/CB	831.76
60 wt. % Fe_3O_4/AC/CB	800.73
Fe_3O_4	38.41

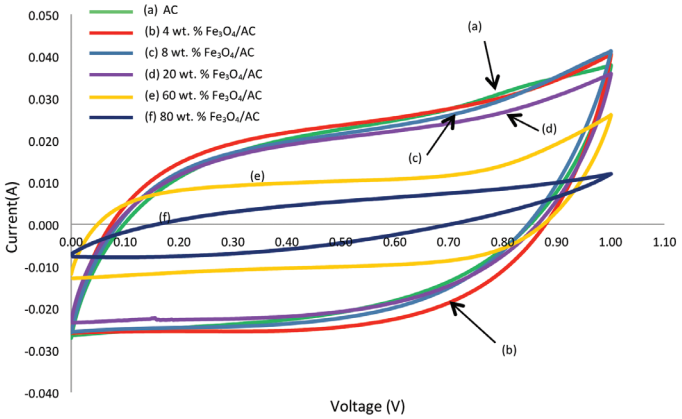

FIGURE 2. Cyclic voltammograms for different compositions of Fe_3O_4 loaded in AC electrodes, scanned at 10 mV/s, in 1 M Na_2SO_3

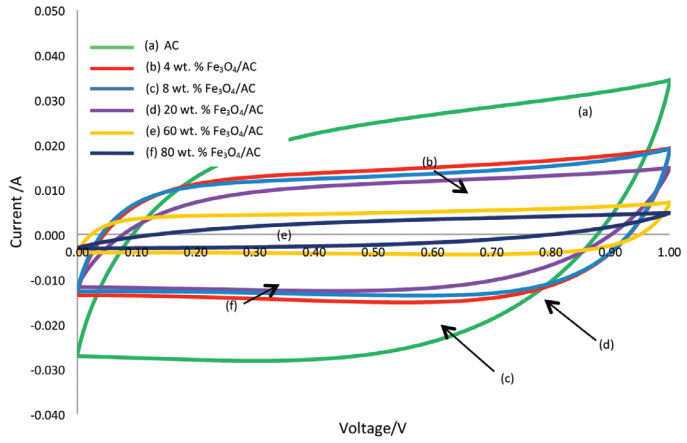

FIGURE 3. Cyclic voltammograms for different compositions of Fe_3O_4 loaded in AC electrodes, scanned at 10 mV/s, in 1 M Na_2SO_4

distinctly different if compared with Na_2SO_3 electrolyte. In fact, the AC electrode is found to exhibit the highest specific capacitance when 1 M Na_2SO_4 solution is adopted as the electrolyte. Nevertheless, there is no obvious redox peaks could be observed for the AC electrodes in both solutions. An implication of these results suggests that the Fe_3O_4 loaded AC composite electrodes and the pure AC electrode may have different storage mechanisms in sulphite and sulphate electrolytes, respectively. Wu et al. (2003) have characterized the capacitive behaviour of Fe_3O_4- carbon black electrodes in several aqueous electrolytes including Na_2SO_3 and Na_2SO_4. The authors suggested that the significant capacitive performance in Na_2SO_3 is attributed from the synergistic effect of both EDLC and the pseudocapacitance which involves successive reduction of the adsorbed sulphite anions. The capacitive current when Na_2SO_4 is used as electrolyte on the other hand is due to the contribution from EDLC mechanism only. Figure 4 shows the specific capacitance of Fe_3O_4/AC composite electrodes as a function of Fe_3O_4 loading, in 1 M Na_2SO_3 and 1 M Na_2SO_4, respectively, at the scan rate of 10 mV/s between 0 and 1V.

Table 2 summarizes the effects of electrolyte and different Fe_3O_4 loading on the specific capacitance of the electrodes. The enhancement of electrochemical storage properties of the AC electrode with a small amount of Fe_3O_4 nanoparticles in Na_2SO_3 is clearly observed, mainly attributed to the synergistic effect of the pseudocapacitance metal oxide with the double layer capacitance AC material. The presence of the Fe_3O_4 nanoparticles could reduce the agglomeration and increase the surface area of AC material electrode. These results are also in good agreement with our observations in SEM (Figure 1) and BET analysis (Table 1). The large porosity of the structure with a higher specific surface area facilitates a better accessibility of the electrolyte inside the bulk of the electrodes during the electrochemical process. In addition to the increase of the effective surface area, a small amount of Fe_3O_4 is also able to supply more electroactive sites for the adsorption/de-adsorption of sulphite (SO_3^{2-}) anions and promotes

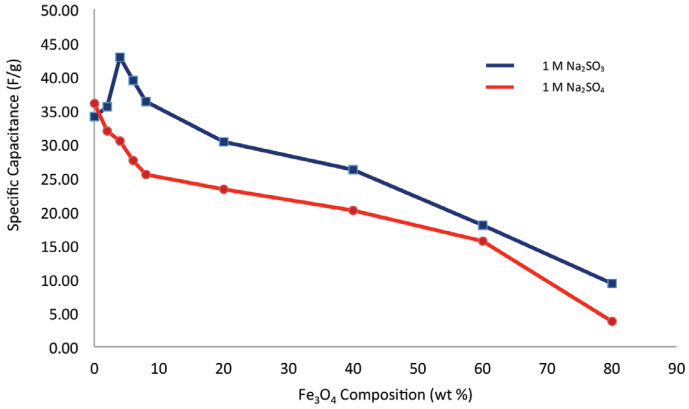

FIGURE 4. Specific capacitance of Fe_3O_4-AC composite electrodes as a function of Fe_3O_4 loading, in 1 M Na_2SO_3 and 1 M Na_2SO_4 respectively, at the scan rate of 10 mV/s between 0 to 1V

TABLE 2. Effects of electrolyte and Fe_3O_4 loading on specific capacitance of Fe_3O_4/AC composite electrodes

Electrode Material	Specific capacitance (F/g)	
	1 M Na_2SO_3	1 M Na_2SO_4
AC	34.08	36.03
2 wt. % Fe_3O_4/AC	35.52	31.96
4 wt. % Fe_3O_4/AC	42.88	30.43
6 wt. % Fe_3O_4/AC	39.45	27.55
8 wt. % Fe_3O_4/AC	36.33	25.50
20 wt. % Fe_3O_4/AC	30.33	23.30
40 wt. % Fe_3O_4/AC	26.22	20.20
60 wt. % Fe_3O_4/AC	18.00	15.60
80 wt. % Fe_3O_4/AC	9.33	3.72

subsequent redox reactions to occur effectively across the interface of electrode-electrolyte.

Nevertheless, as clearly indicated in Figure 4, the further increase in Fe_3O_4 content within the range 20 – 60 wt. % starts deteriorating the capacitive behaviour of the composite electrodes. The decrease in specific capacitance could be attributed to the low conductivity of Fe_3O_4 nanoparticles in large amount, which in turn increase the equivalent series resistance (ESR) of the electrode. The specific capacitances of pure Fe_3O_4 electrodes were found to be less than 9.4 and 4.0 F/g in Na_2SO_3 and Na_2SO_4 respectively, which clearly dictates its poor capacitive performance. Our observations are well complement with the similar effort by Wu et al. (2003). They reported that Fe_3O_4 has a very poor conductivity and preliminary tests showed that it was necessary to combine the iron oxide with some conductive additives in order to significantly enhance its capacitive performance.

On top of low conductivity of Fe_3O_4, a fade in capacitance with increasing Fe_3O_4 could be also due to the particle agglomeration, as shown in Figure 1(e) and 1(f). This phenomenon is similar to another investigation on the hydrous RuO_2-AC composite electrode, which a significant distortion on the capacitive behaviour is observed for the electrode with more than 40 wt. % RuO_2 loading (Kim & Popov 2002). Since ion diffusion through the active materials controls the redox reactions of the electrode, the diffusive capability of these materials will decrease with increasing of the particle size. Under such circumstances, the ions thus require longer time to reach the entire electrodes. In addition, the agglomeration of the metal oxide nanoparticles will reduce the porosity of the electrode material, which in turn distorts the effective surface area that is available for the redox process. Similar trend has been observed by Dubal et al. (2012) for galvanostatically deposited Fe doped MnO_2 thin films. The low porosity of composite electrodes contributes to the poor diffusive capability since the large Fe_3O_4 precipitates agglomerated on the AC surface and block most of the pores, preventing the ions to diffuse into the inner pores of the electrodes.

ELECTROCHEMICAL IMPEDANCE SPECTROSCOPY (EIS)

The EIS measurement was carried out on AC and Fe_3O_4 /AC composite electrodes in the frequency range of 10^4 to 10^{-2} Hz. Figure 5 shows the Nyquist plots of AC impedance of the composite electrodes with different

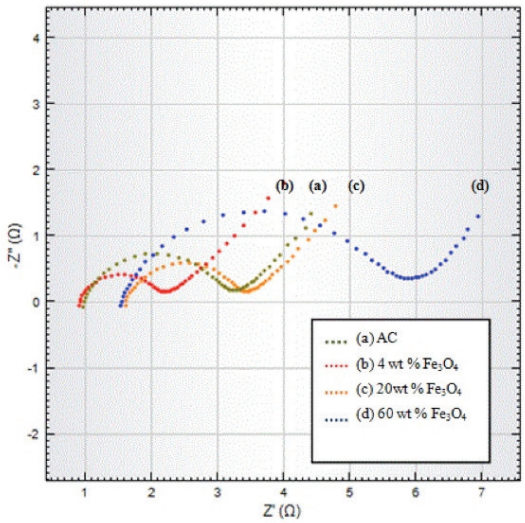

FIGURE 5. Nyquist plots obtained for composite electrodes with different Fe_3O_4 loading, at 1 V over the frequency range of 100 kHz - 100 mHz in 1 M Na_2SO_3

Fe_3O_4 compositions in Na_2SO_3. It can be seen that all the impedances consist of an arc and a slanted line at low frequency. In the high frequency region, the intercept of the semicircle on the real axis of the Nyquist spectrum represents the solution resistance (R_{sol}) which provides the ohmic resistance of the electrolyte and the internal resistance of the electrode materials. The semicircles in the high- and mid-frequency regions are attributed to the charge transfer resistance at the interface of the Fe_3O_4-Fe_3O_4, AC-Fe_3O_4, AC-AC composite and the Na_2SO_3 electrolyte. The electron transfer which occurs in these regions during the charge/discharge processes is modelled by an interfacial charge transfer resistance (R_{ct}) or polarisation resistance (R_p). After the semicircle, the Nyquist spectrum shows a long tail in the low-frequency region pertaining to the Warburg resistance or the diffusion of ions into the bulk of the electrode. As shown in Figure 5, it is apparent that the sizes (diameter) of the Nyquist semicircles are varied for the electrodes with different Fe_3O_4 composition. When Na_2SO_3 is used as an electrolyte, the R_{ct} for the electrodes with different Fe_3O_4 composition is found to decrease in the order of 4.28 Ω (60 wt. %), 1.87 Ω (20 wt. %) and 1.37 Ω (4 wt. %). On the other hand, the R_{ct} of the pure AC electrode is found to be 2.30 Ω. From these results, it is clear that the 4 wt. % Fe_3O_4 /AC composite electrode exhibits the lowest R_{ct} value, consistent with the smallest size (diameter) of the Nyquist semicircle within the high frequency region. A reduction in the value of R_{ct} implies that the surface modification by addition of fairly small amount of Fe_3O_4 can enhance the conductivity of the composite electrode and hence improves its capacitive performance, in agreement with the results obtained from CV analysis.

The fitting of the impedance expressions obtained from the equivalent circuit to the experimental Nyquist spectra was performed using the NOVA equivalent circuit editor in order to determine the most representative physical processes that taking place in the systems under investigation (Figure 6). In the present study, the double layer capacitor in EIS experiments often behaves like constant-phase element (CPE) as a result of imperfection on the real electrochemical cell including surface roughness, leaky capacitor and non-uniform current distribution (Jovic 2012). The negative phase at high frequencies shows the effect of inductance error (L) on the impedance spectra of an electrochemical cell attributed to the improper length of lead and wiring configuration (MacDonald & Barsoukov 2005).

Table 3 summarises the equivalent circuit parameters obtained from the fitting results in 1 M Na_2SO_3. From the table, it is found that 4 wt. % Fe_3O_4 in the composite electrode shows relatively lower R_Ω (0.83 Ω) and R_{ct} (1.37 Ω) in comparison to R_Ω (0.90 Ω) and R_{CT} (2.30 Ω) of pure AC electrode. A reduced value of R_{CT} implies that the surface modification with very small amount of Fe_3O_4 enhances the conductivity of the composite electrodes. Additionally, Warburg impedance (W) of 4 wt. % Fe_3O_4 shows a much lower value compared to pure AC electrode, which corresponds to more vertical line leaning to the imaginary axis at a low frequency region. Similar EIS investigations were reported in other studies as well (Masarapu et al. 2009; Wang et al. 2012) showing that enhanced capacitive performance is related to lower Warburg impedance values. These findings show that 4 wt. % Fe_3O_4 demonstrates more ideal capacitive behaviour due to more facile electrolyte diffusion to the composite surface.

In general, porous electrodes generate an exponent value of n = 0.5 while rough electrode possesses n value between 0.5 and 1 (Masarapu et al. 2009). In this

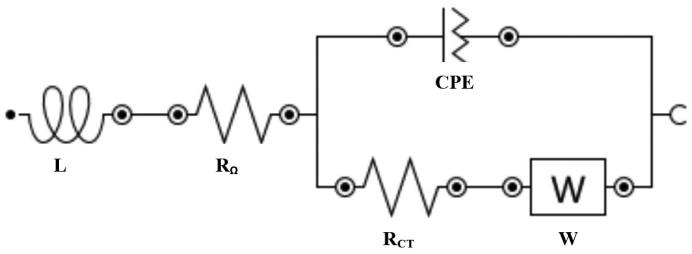

FIGURE 6. The equivalent circuit used to fit the Nyquist spectra using NOVA equivalent circuit editor

TABLE 3. Simulated values of L. R_Ω, R_{CT}, CPE, W, n from the equivalent circuit in Figure 6

Electrode composition	Inductance, L (nH)	Solution resistance , R_Ω (Ω)	Charge transfer resistance, R_{CT} (Ω)	Constant-phase element, CPE (μMho)	Warburg element, W (mMho)	Exponent (n)
AC	282	0.90	2.30	475	685	0.723
4 wt. % Fe_3O_4	230	0.83	1.37	772	487	0.695
20 wt. % Fe_3O_4	235	1.55	1.87	583	622	0.710
60 wt. % Fe_3O_4	274	1.48	4.28	452	519	0.727

case, it can be observed that the values of *n* increase with increasing Fe_3O_4 loading. The higher value of the exponent in 20 and 60 wt. % Fe_3O_4 shows that these composite electrodes are behaving as typical non-porous electrodes in which the ion diffusion is taking place only on the surface of the composite electrodes. These findings are consistent with SEM micrographs (Figure 1) and BET surface area measurement (Table 1) on composite electrodes with different Fe_3O_4 loading. The non-porous nature limits the number of ions that diffuse into the bulk of electrodes and thus yields lower specific capacitance compared to the porous electrodes.

CONCLUSION

The capacitive performance of Fe_3O_4 -AC nanocomposite electrode materials in Na_2SO_3 and Na_2SO_4 has been characterized. The highest specific capacitance of 43 F/g is achieved with a relatively low Fe_3O_4 loading (4 wt. %) in 1 M Na_2SO_3. However, bulk increasing of the Fe_3O_4 content is found to distort the capacitive performance and deteriorate the specific surface area of the electrode, mainly due to the aggregation of the Fe_3O_4 particles within the composite. Additionally, the Fe_3O_4-AC nanocomposite electrode in Na_2SO_3 electrolyte exhibits a better charge storage performance if compared with Na_2SO_4 solution. It is believed that Fe_3O_4 nanoparticles can provide favourable surface adsorption sites for sulphite (SO_3^{2-}) anions during the redox and intercalation reactions. The improvement of the capacitive performance of the 4 wt. % Fe_3O_4 –AC composite electrode is believed attributed to the contribution of synergistic effect of EDLC and pseudocapacitance charge storage mechanism, as well as the enhancement on the specific surface areas of the electrode.

ACKNOWLEDGEMENTS

The authors would like to acknowledge the financial support from the FRGS research grants, Ministry of Education (MOE), Malaysia (Projects No.: FRGS/2/2010/SG/UNIM/02/1 & FRGS/2/2010/ST/UNIM/03/2), HIR-Chancellory UM (J-21002-73810) and HIR-MOHE (UM.C/625/1/HIR/MOHE/SC/06). All the research facilities from the Faculty of Engineering (University of Nottingham Malaysia Campus) and Materials Engineering Division, School of Technology (College Tunku Abdul Rahman) are very much appreciated as well.

REFERENCES

Belanger, D., Brousse, T. & Long. J. 2008. Manganese oxides: Battery materials make the leap to electrochemical capacitors. *The Electrochemical Society's Interface* 17(1): 49-52.

Brousse, T. & Belanger. D. 2003. A hybrid Fe_3O_4-MnO_2 capacitor in mild aqueous electrolyte. *Electrochemical and Solid-State Letters* 6: A244-A248.

Chen, J., Huang, K. & Liu, S. 2009. Hydrothermal preparation of octadecahedron Fe_3O_4 thin film for use in an electrochemical supercapacitor. *Electrochimica Acta* 55: 1-5.

Conway, B.E., Birss, V. & Wojtowicz, J. 1997. The role and utilization of pseudocapacitance for energy storage by supercapacitors. *Journal of Power Sources* 66: 1-14.

Cottineau, T., Toupin, M., Delahaye, T., Brousse, T. & Belanger, D. 2005. Nanostructured transition metal oxides for aqueous hybrid electrochemical supercapacitors. *Applied Physics A* 82: 599-606.

Dubal, D.P., Kim, W.B. & Lokhande, C.D. 2012. Galvanostatically deposited Fe: MnO2 electrodes for supercapacitor application. *Journal of Physics and Chemistry of Solids* 73: 18-24.

Du, X., Wang, C., Chen, M., Jiao, Y. & Wang, J. 2009. Electrochemical performances of nanoparticle Fe_3O_4/ Activated carbon supercapacitor using KOH electrolyte solution. *Journal of Physical Chemistry C* 113: 2643-2646.

Ganesh, V., Pitchumani, S. & Lakshminarayanan, V. 2006. New symmetric and asymmetric supercapacitors based on high surface area porous nickel and activated carbon. *Journal of Power Sources* 158: 1523-1532.

Hu, C.C., Liu, M.J. & Chang, K.H. 2007. Anodic deposition of hydrous ruthenium oxide for supercapacitors. *Journal of Power Sources* 163: 1126-1131.

Hu, C.C. & Chen, W.C. 2004. Effects of substrates on the capacitive performance of $RuO_x \cdot nH_2O$ and activated carbon - RuO_x electrodes for supercapacitors. *Electrochimica Acta* 49: 3469-3477.

Jayalakshmi, M., Rao, M.M., Venugopal, N. & Kim, K-B. 2007. Hydrothermal synthesis of SnO_2-V_2O_5 mixed oxide and electrochemical screening of carbon nano-tubes (CNT), V_2O_5 , V_2O_5 - CNT , and SnO_2 - V_2O_5 - CNT electrodes for supercapacitor applications. *Journal of Power Sources* 166: 578-583.

Jovic, V.D. 2012. Determination of the correct value of Cdl from the impedance results fitted by the commercially available software. http://www.gamry.com Accessed on Jan 2012.

Kalpana, D., Omkumar, K.S., Kumar, S.S. & Renganathan, N.G. 2006. A novel high power symmetric ZnO/carbon aerogel composite electrode for electrochemical supercapacitor. *Electrochimica Acta* 52: 1309-1315.

Kim, H. & Popov, B.N. 2002. Characterization of hydrous ruthenium oxide/carbon nanocomposite supercapacitors prepared by a colloidal method. *Journal of Power Sources* 104: 52-61.

Kim, Y.H. & Park, S.J. 2011. Roles of nanosized Fe_3O_4 on supercapacitive properties of carbon nanotubes. *Current Applied Physics* 11: 462-466.

Kuo, S.L. & Wu, N.L. 2003. Composite supercapacitor containing tin oxide and electroplated ruthenium oxide. *Electrochemical Solid State Letter* 6: A85-A87.

Lee, H.Y. & Goodenough, J.B. 1999. Supercapacitor behaviour with KCl electrolyte. *Journal of Solid State Chemistry* 223: 220-223.

Lu, T., Zhang, Y., Li, H., Pan, L., Li, Y. & Sun, Z. 2010. Electrochemical behaviours of graphene – ZnO and graphene – SnO_2 composite films for supercapacitors. *Electrochimica Acta* 55: 4170-4173.

Macdonald, J.R. & Barsoukov, E. 2005. *Impedance Spectroscopy, Theory Experiment and Applications*. Canada: John Wiley & Sons, Inc.

Mallouki, M., Tran-Van, F., Sarrazin, C., Simon, P., Daffos, B., De, A., Chevrot, C. Fauvarque, J. 2006. Polypyrrole-Fe_2O_3 nanohybrid materials for electrochemical storage. *Journal of Solid State Electrochemistry* 11: 398-406.

Masarapu, C., Zeng, H.F., Hung, K.H. & Wei, B. 2009. Effect of temperature on the capacitance of carbon nanotube supercapacitors. *ACS Nano* 3: 2199-2206.

Nagarajan, N., Humadi, H. & Zhitomirsky, I. 2006. Cathodic electrodeposition of MnO_x films for electrochemical supercapacitors. *Electrochimica Acta* 51: 3039-3045.

Nagarajan, N. & Zhitomirsky, I. 2006. Cathodic electrosynthesis of iron oxide films for electrochemical supercapacitors. *Journal of Applied Electrochemistry* 36: 1399-1405.

Nathan, T., Aziz, A., Noor, A.F. & Prabaharan, S.R.S. 2008. Nanostructured NiO for electrochemical capacitors: Synthesis and electrochemical properties. *Journal of Solid State Electrochemistry* 12: 1003-1009.

Pasquier, A.D., Plitz, I., Gural, J., Menocal, S. & Amatucci, G. 2003. Characteristics and performance of 500 F asymmetric hybrid advanced supercapacitor prototypes. *Journal of Power Sources* 113: 62-71.

Sassin, M.B., Mansour, A.N., Pettigrew, K.A., Rolison, D.R. & Long, J.W. 2010. Electroless deposition of conformal nanoscale iron oxide on carbon charge storage. *ACS Nano* 4: 4505-4514.

Shukla, A.K., Sampath, S. & Vijayamohanan, K. 2000. Electrochemical supercapacitors: Energy storage beyond batteries. *Current Science* 79: 1656-1661.

Simon, P. & Gogotsi, Y. 2008. Materials for electrochemical capacitors. *Nature Materials* 7: 845-854.

Wang, H., Tang, Z.Y., Sun, L., He, Y.B., Wu, Y.X. & Li, Z.Y. 2009. Capacitance performance enhancement of TiO_2 doped with Ni and graphite. *Rare Metals* 28: 231-236.

Wang, S.C., Chen, C.Y., Chien, T.C., Lee, P.Y. & Lin, C.K. 2008. Supercapacitive properties of spray pyrolyzed iron-added manganese oxide powders deposited by electrophoretic deposition technique. *Thin Solid Films* 517: 1234-1238.

Wang, S.Y., Ho, K.C., Kuo, S.L. & Wu, N.L. 2006. Investigation on capacitance mechanisms of Fe_3O_4 electrochemical capacitors. *Journal of the Electrochemical Society* 153: A75-A80.

Wang, X., Han, X., Lim, M., Singh, N., Gan, C.L., Jan, M. & Lee, P.S. 2012. Nickel cobalt oxide-single wall carbon nanotube composite material for superior cycling stability and high-performance supercapacitor application. *The Journal of Physical Chemistry C* 116: 12448-12454.

Wu, N.L., Wang, S.L. & Han, C.Y. 2003. Electrochemical capacitor of magnetite in aqueous electrolytes. *Journal of Power Sources* 113: 173-178.

Wu, N.L. 2002. Nanocrystalline oxide supercapacitors. *Materials Chemistry and Physics* 75: 6-11.

Xie, K.Y., Li, J., Lai, Y.Q., Lu, W., Zhang, Z.A., Liu, Y.X., Zhou, L.M. & Huang, H.T. 2011. Highly ordered iron oxide nanotube arrays as electrodes for electrochemical energy storage. *Electrochemistry Communications* 13: 657-660.

Yeong, J., Liang, K., Hyeok, K. & Hee. Y. 2005. Nickel oxide/carbon nanotubes nanocomposite for electrochemical capacitance. *Synthetic Metals* 150: 153-157.

Yuan, G.H., Jiang, Z.H., Aramata, A. & Gao, Y.Z. 2005. Electrochemical behaviour of activated-carbon capacitor material loaded with nickel oxide. *Carbon* 43: 2913-2917.

Zhang, S.W. & Chen, G.Z. 2008. Manganese oxide based materials for supercapacitors. *Energy Materials: Materials Science and Engineering for Energy Systems* 3: 186-200.

M.Y. Ho, P.S. Khiew*, D. Isa & T.K.Tan
Faculty of Engineering
University of Nottingham Malaysia Campus
Jalan Broga, 43500 Semenyih, Selangor
Malaysia

M.Y. Ho
Materials Engineering Division, School of Technology
Tunku Abdul Rahman College
Jalan Genting Kelang, 53300 Kuala Lumpur
Malaysia

W.S. Chiu
Low Dimensional Materials Research Center
Department of Physics, Faculty of Science
University Malaya
50603 Kuala Lumpur
Malaysia

C.H. Chia, M.A.A. Hamid & R. Shamsudin
School of Applied Physics, Faculty Science and Technology
Universiti Kebangsaan Malaysia
43600 Bangi, Selangor
Malaysia

*Corresponding author; email: PoiSim.Khiew@nottingham.edu.my

Received: 15 March 2013
Accepted: 20 December 2013